ELSEVIER

Journal of Pharmaceutical and Biomedical Analysis
26 (2001) 701–716

JOURNAL OF
PHARMACEUTICAL
AND BIOMEDICAL
ANALYSIS

www.elsevier.com/locate/jpba

In vitro metabolism studies of the prodrug, 2′,3′,5′-triacetyl-6-azauridine, utilizing an automated analytical system

J. Zhou [1], C.M. Riley *, R.L. Schowen

Department of Pharmaceutical Chemistry and the Center for BioAnalytical Research, University of Kansas, Lawrence, KS 66045, USA

Received 21 June 2000; received in revised form 13 March 2001; accepted 18 March 2001

Abstract

The purpose was to study in vitro metabolism of 2′,3′,5′-triacetyl-6-azauridine (**1**) by porcine liver esterase (PLE) and in human plasma using an automated analytical system developed previously. A gradient-LC method was developed to study the concentration-time course of **1** and its metabolites. A fast-LC assay was used to study the temperature effect on the metabolism of **1** by the PLE. **1** and all of its proposed possible metabolites were separated by the gradient-LC method in less than 10 min. Two simplified kinetic schemes were developed to describe the time course of **1**, the intermediates and final metabolites with only five rate constants for the metabolisms of **1** by PLE and four rate constants in human plasma. Both enthalpy and entropy of activation in the in vitro metabolism of **1** by PLE were obtained.

Keywords: 2′,3′,5′-Triacetyl-6-azauridine; In vitro metabolism; Prodrug; Automation; Reversed-phase chromatography; Microdialysis

1. Introduction

2′,3′,5′-Triacetyl-6-azauridine (**1**) is an orally active prodrug of the anti-psoriasis and anti-neoplastic drug 6-azauridine (**2**) [1–3]. The chemical stability of **1** was studied previously and a simplified kinetic scheme (Fig. 1) has been developed and reported [4]. The chemical (non-enzymatic) degradation of **1** to its final product, **2**, involves (a) the conversion of **1** (T) to the pool of primary–secondary diacetates PSD (**4b** and **4c**) and the secondary–secondary diacetate SSD (**4a**); (b) conversion of PSD to the primary monoacetate PM (**5c**) and the pool of secondary monoacetates

* Corresponding author. Present address: Dupont Pharmaceutical Company, Analytical Research and Development, Experimental Station E353, Dupont Pharmaceuticals Company, P.O. Box 80353, RT 141 and Henry Clay Road, Wilmington, DE 19880-0353, USA. Tel.: +1-302-6957122; fax: +1-302-6953230.

E-mail address: christopher.m.riley@dupontpharma.com (C.M. Riley).

[1] Present address: Alza Corporation, Building M3, 1010 Joaquin Road, P.O. Box 7210, Mountain View, CA 94039-7210, USA.

0731-7085/01/$ - see front matter
PII: S0731-7085(01)00433-2

SM (**5a** + **5b**), along with conversion of SSD to SM; and (c) conversion of PM and **SM** to the nucleoside **N** (**2**, 6-azauridine). However, the in vitro metabolism of **1** has so far not been reported yet.

Although the maturity of HPLC technology has provided a vital tool for investigating in vitro drug metabolism, manual sampling procedures are time-consuming and labor intensive. In addition, multiple sample preparation steps may introduce human error in preparing large number of samples which will inevitably compromise the quality of the data. Recently, an automated analytical system using microdialysis as a sampling technique has been developed for enzyme kinetic studies [5]. The system has been proven to be rugged and easy to use with good precision ($< 4\%$ RE) and accuracy ($< 5\%$ RSD). This paper describes the continued use of this automated analytical system in the studies of in vitro metabolism of **1** by porcine liver esterase (PLE) and in human plasma.

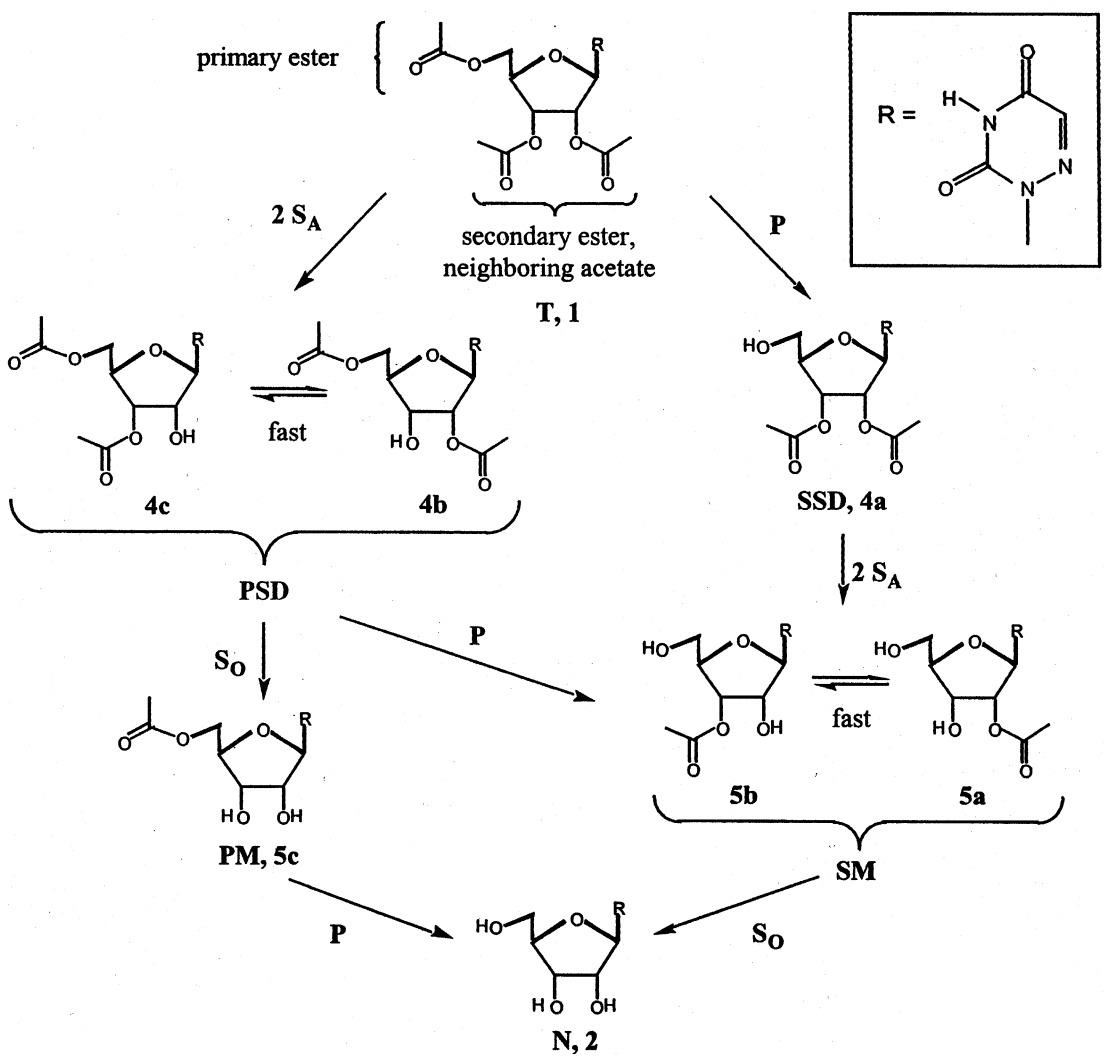

Fig. 1. Simplified kinetic scheme for the non-enzymatic hydrolysis of 2′,3′,5′-triacetyl-6-azauridine (**1**). Adapted from [4].

2. Materials and methods

2.1. Materials

2′,3′,5′-Triacetyl-6-azauridine was a gift from Dr William Drell, U.R. Laboratories, La Jolla, CA. Porcine liver esterase (PLE, EC 3.1.1.1), *p*-nitrophenyl acetate (PNPA), *p*-nitrophenol (PNP, spectrophotometric grade), 6-azauridine, 6-azauricil (**3**), and sodium hydroxide were obtained from Sigma Chemical Co. (St. Louis, MO). All water was deionized with a Nanopure II Water Deionization System from Barnstead/Thermolyne (Boston, MA). *o*-Phosphoric acid (85%), sodium dihydrogen phosphate, disodium monohydrogen phosphate, hydrochloric acid and sodium chloride were reagent grade. Acetonitrile (ACN) and methanol (MeOH) were HPLC grade. All were purchased from Fisher Scientific (Fair Lawn, NJ).

2.2. Apparatus

The automated analytical system consisted of a thermostated reaction vessel connected to an autotitrator, a microdialysis sampling system and a liquid chromatograph as shown in Fig. 2. A 50 ml drug solution was placed in a 100 ml customized water jacketed reaction vessel (cat. No. 5340-972, ACE Glass Incorporated, Vineland, NJ), thermostated (± 0.2°C) using a Fisher Scientific (Pittsburgh, PA) Model 801 Isotemp Constant Temperature Circulator. A Metrohm (Herisau, Switzerland) Model 632 pH meter was used with Model 655 Dosimat and Model 614 Impulsomat in stat-mode to maintain the pH of the reaction mixture. The sampling system consisted of a BAS (West Lafayette, IN) DL-5 microdialysis probe (30 000 Da MW cutoff) mounted radially across the reaction vessel (Fig. 3) and a Harvard Apparatus (South Natick, MA) Model 44 infusion

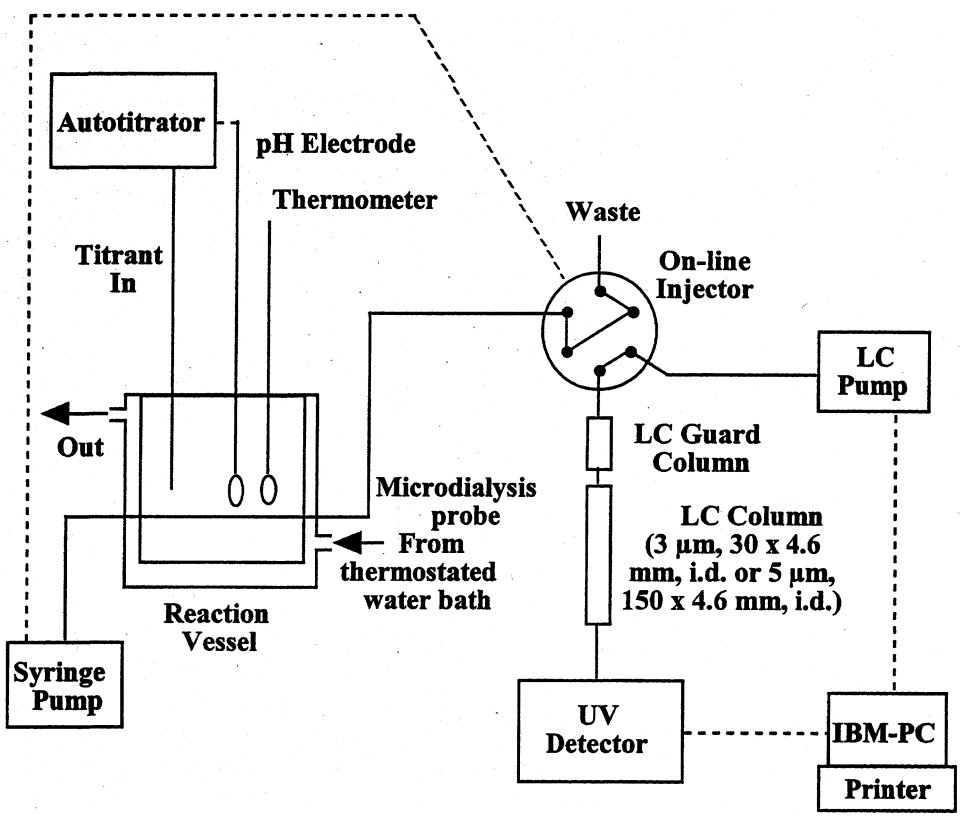

Fig. 2. Diagram of the automated system for the studies of **1** in vitro metabolism.

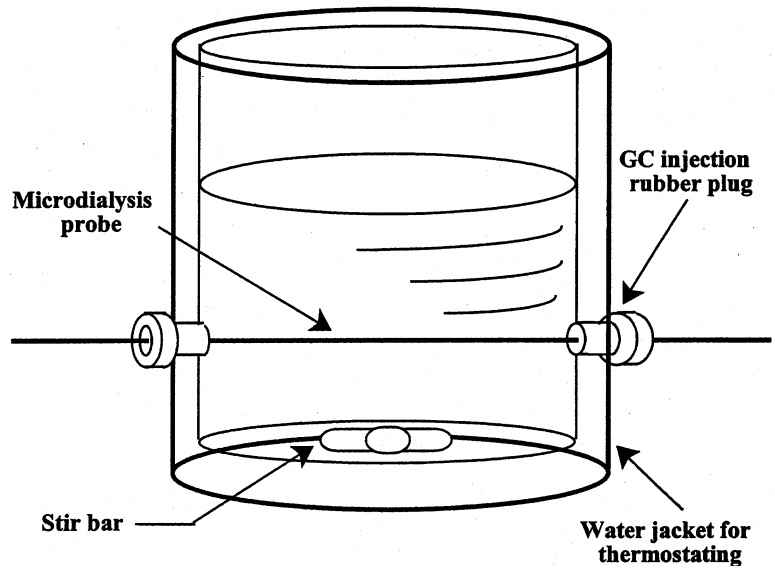

Fig. 3. Diagram of the DL-5 probe mounted radially across the customized, water-jacked reaction vessel. The inlet and outlet of the reaction vessel for mounting the microdialysis probe were sealed with gas chromatography (GC) injection rubber plug. Adapted from J.M. Ault, PhD. Dissertation in Pharmaceutical Chemistry, University of Kansas (1994).

pump for continuous perfusion of the probe. The dialysate was perfused into a 2 μl injection loop on a Valco Instrument (Houston, TX) Model EF-60 on-line injector. The injector was equipped with an electrical actuator for rapid sampling and was controlled by the signal from the infusion pump. The LC system consisted of a Beckman (Fullerton, CA) 126 Programmable Solvent Module and 168 Diode Array Detector Module, both of which were controlled through an IBM (Armonk, NY) PS/2 Model 56SX computer with Beckman System Gold Chromatography Software, connected to an Epson (Torrance, CA) LQ-570 printer. A 30×4.6 mm, 3 μm ODS Hypersil column from Keystone (Bellefonte, PA) was used to perform the fast separation of **1**, and a 150×4.6 mm, 5 μm ODS Hypersil column from Sigma Chemical Co. (St. Louis, MO) was purchased to separate **1** and all of its deacetylated products with a gradient method. Both columns were protected by an ODS Hypersil guard column (10×4.6 mm, 5 μm) from Sigma Chemical Co.

2.3. Buffers and solutions

2.3.1. Buffers

Phosphate buffer (pH 6.79, 25 mM NaH_2PO_4 and 25 mM Na_2HPO_4) was used in all **1** studies with sodium chloride added to adjust the ionic strength to 0.50. The buffer was prepared weekly and stored in a refrigerator at 1°C.

2.3.2. Microdialysis perfusate

Phosphate buffer (pH 6.40, 1.0 M) was used as microdialysis perfusate for the fast separation of **1** and its metabolites. The perfusate was later switched to the above described phosphate buffer (pH 6.79, 50 mM) in the kinetic studies of the metabolites with PLE and in human plasma using a gradient separation method. The concern was that due to the prolonged sampling intervals (15 min, due to the LC assay time) and thus the long time of the kinetic run ($\sim$4–6 h comparing to $\sim$20 min kinetic run with the fast LC assay), a significant amount of the phosphate buffer might be able to leak into the reaction medium to perturb the reaction.

2.3.3. Titrant in pH-stat

MeOH–NaOH (0.50 N) solution (4:96, v/v) was used as titrant for the kinetic studies with PLE. HCl (1.0 N) solution was used to maintain the pH of the plasma during its kinetic runs. Both solutions were prepared semi-annually and stored at room temperature.

2.3.4. Enzyme solutions

Partially purified PLE (Sigma cat. No. E2884) was used in the studies of **1**. A 3 ml aliquot of the esterase suspension (~ 40 mg/ml in 3.2 M $(NH_4)_2SO_4$ solution) was diluted to 15 ml with 50 mM phosphate buffer (pH 6.79). After it was centrifuged at 1000 × *g* for 5 min, the supernatant was saved and stored in a refrigerator at 1°C. This solution was used as it was or further diluted when necessary. The stability of the enzyme and the activity of each enzyme preparation were assessed by the method of Zhou et al. [6]. The concentration of PLE was calculated based upon a molecular weight of 163 000 and absorbance (1 mg/ml) of 1.305 at 280 nm [7]. The prepared PLE solution has a stability of at least 2 days [5].

2.3.5. Human plasma

Fresh human blood was collected from a consenting healthy adult in heparinized tubes and centrifuged at 450 × *g* for 15 min [8]. The supernatant was saved and stored in a freezer (below − 16°C) since collection. The frozen human plasma collected on four separate occasions over a period of 5 months was thawed and pooled together before experiments, and was centrifuged at 1000 × *g* for 10 min using a Dynac Centrifuge from Clay Adams (Parsippany, NJ) to get rid of the small amount of precipitation. The supernatant was then saved for experiments.

2.3.6. Stock solutions

1(~ 30 mg) was weighted and dissolved in 200 ml (~ 0.4 mM) MeOH–phosphate buffer (pH 6.79, 50 mM) (4:96, v/v) immediately before the kinetic experiments with PLE. For human plasma experiments, **1** (~ 0.15 g) was dissolved in 1 ml MeOH in a 25 ml volumetric flask to ensure complete dissolution, and then phosphate buffer (pH 6.79, 50 mM) was added to volume to make a stock solution (~ 16 mM).

*2.3.7. Mixture of **1** and its deacetylated products*

1 (~ 0.12 g) was dissolved in water (~ 200 ml). NaOH solution (0.8 N) was added to adjust the pH to 11.5 and more NaOH solution was added when desired. The concentrations of **1** and its deacetylated products were monitored by a LC gradient method once every hour until significant concentrations of each component were obtained. This mixture was then used to prepare a solution (200 ml) of phosphate buffer (50 mM)–MeOH (96:4, v/v) with ionic strength adjusted to 0.5 using NaCl and pH adjusted to 7.50.

2.4. Experimental procedures

*2.4.1. Recovery studies of **1** by fast-LC*

A known concentration of 50 ml of **1** (an average concentration of 0.26 mM) was placed in the isothermal reaction vessel. The pH of the solution was adjusted to 7.50 by the pH-stat. The microdialysis probe was submersed in the solution and perfused with phosphate buffer (pH 6.40) at a flow rate between 4 and 24 μl/min. The sample from the probe was perfused into the LC injector and the perfusion pump was programmed to send a signal to the injector for injection at certain time intervals. The concentrations inside the probe measured by the fast LC method were used to calculate the relative recovery.

*2.4.2. Recovery studies of **1** and its deacetylated products by a gradient LC method*

A mixture (50 ml) of **1** and its deacetylated products was placed in the isothermal reaction vessel. The microdialysis probe was submersed in the solution and perfused with phosphate buffer (pH 6.79) at a flow rate between 2 and 12 μl/min. The sample from the probe was perfused into the LC injector and was analyzed by the LC gradient method. An aliquot of the mixture was also perfused directly into the LC injector to measure the concentrations of the each component in the mixture. The concentrations of each component measured inside and outside the probe were used to calculate the recovery of that component. Both recovery studies were conducted at various temperatures between 30.0 and 39.0°C.

2.4.3. Kinetic studies with PLE

A known concentration of 50 ml of **1** (~ 0.26–0.4 mM) was placed in the isothermal reaction vessel. The pH of the solution was adjusted to and kept at 7.50 by the pH-stat. The microdialysis probe was submersed in the solution and perfused with phosphate buffer either at pH 6.40 when coupling with a fast-LC method or at 6.79 when coupling with a LC gradient method. The reaction was initiated by adding 1 ml of 8 mg/ml (when using the fast-LC method) or 0.4 mg/ml PLE solution (when using the gradient method). A sample was injected every 45 s for the fast-LC method and every 15 min for the gradient method. All reactions were monitored for at least three half-lives of **1** in its apparent first-order decay.

2.4.4. Kinetic studies with human plasma

An aliquot (50 ml) of the human plasma was placed in the isothermal reaction vessel. The pH of the plasma was adjusted to and kept at 7.40 by the pH-stat. The microdialysis probe was submersed in the plasma and perfused with phosphate buffer (pH 6.79). The reaction was initiated by adding an aliquot (1.0 ml) of a known concentration of **1** (16 mM) stock solution. The microdialysis samples were injected every 15 min and the concentrations of the **1** and its metabolites were monitored for more than 300 min.

3. Results

3.1. HPLC assay development and validation

A LC assay based on the method of Riley et al. [4], employing gradient elution with a run time of 15 min, was developed to separate and quantify **1** and all its metabolites. Two microliters of sample was injected into the system by overfilling the injector loop, and the appearance and disappearance of the **1** and its metabolites was followed over time. The flow rate was 1.0 ml/min and UV detection was at 254 nm. Mobile phase A was 100% phosphate buffer (pH 3.00, 50 mM) and mobile phase B was ACN–phosphate buffer (pH 3.00, 50 mM) (80:20, v/v). The gradient profile was 100% A for 0.5 min, ramped from 0% B at 0.5 min to 100% B at 8.5 min, then to 100% A at 9.5 min and reequilibrated for 5.5 min. The helium sparging unit was critical to obtaining a stable baseline. Fig. 4 shows a LC chromatogram of the gradient separation of **1** and its metabolites.The linearity of the chromatographic system was determined over the range 16–326 μM for **1**, 26–524 μM for **2**, and 51–1023 μM for **3** (an in vivo metabolite of **2**) by manual injection of authentic standards of **1**, **2** and **3** in phosphate buffer (pH 6.79) at six levels of concentrations. Each solution was injected in duplicate. The mean peak areas (A_P) of **1**, **2** and **3** were related to the concentration injected by the following equations:

$$A_P = (1.904 \pm 0.007 \times 10^{-2})\ [\mathbf{1}] + (2.059 \pm 1.506 \times 10^{-3})$$
$$n = 6 \quad r^2 = 1.000 \qquad (1)$$

$$A_P = (1.876 \pm 0.004 \times 10^{-2})\ [\text{6-Azauridine}] + (1.463 \pm 1.438 \times 10^{-2})$$
$$n = 6 \quad r^2 = 1.000 \qquad (2)$$

$$A_P = (1.774 \pm 0.005 \times 10^{-2})\ [\text{6-Azauracil}] + (3.236 \pm 3.165 \times 10^{-2})$$
$$n = 6 \quad r^2 = 1.000. \qquad (3)$$

The fact that the values of the slopes of these three linear curves were very close indicated that these three compounds have very similar absorptivities. The intercept was less than 0.2% of the peak area at the highest standard concentration (325.6 μM for **1**, 523.7 μM for 6-azauridine and 1023 μM for 6-azauracil). The reproducibility of the assay was determined at the lowest and highest concentration levels in the linearity study as shown in Table 1. Six samples were individually prepared at each concentration, and each sample was injected once. The fast-LC method and its validation have been reported previously [5].

*3.2. Kinetic modeling of the in vitro metabolism of **1** by PLE*

Fig. 5 shows the course of appearance and disappearance of the metabolites of **1** by PLE (58.3 nM) at pH 7.50 and 30°C. Three diesters (**4a**, **4b**

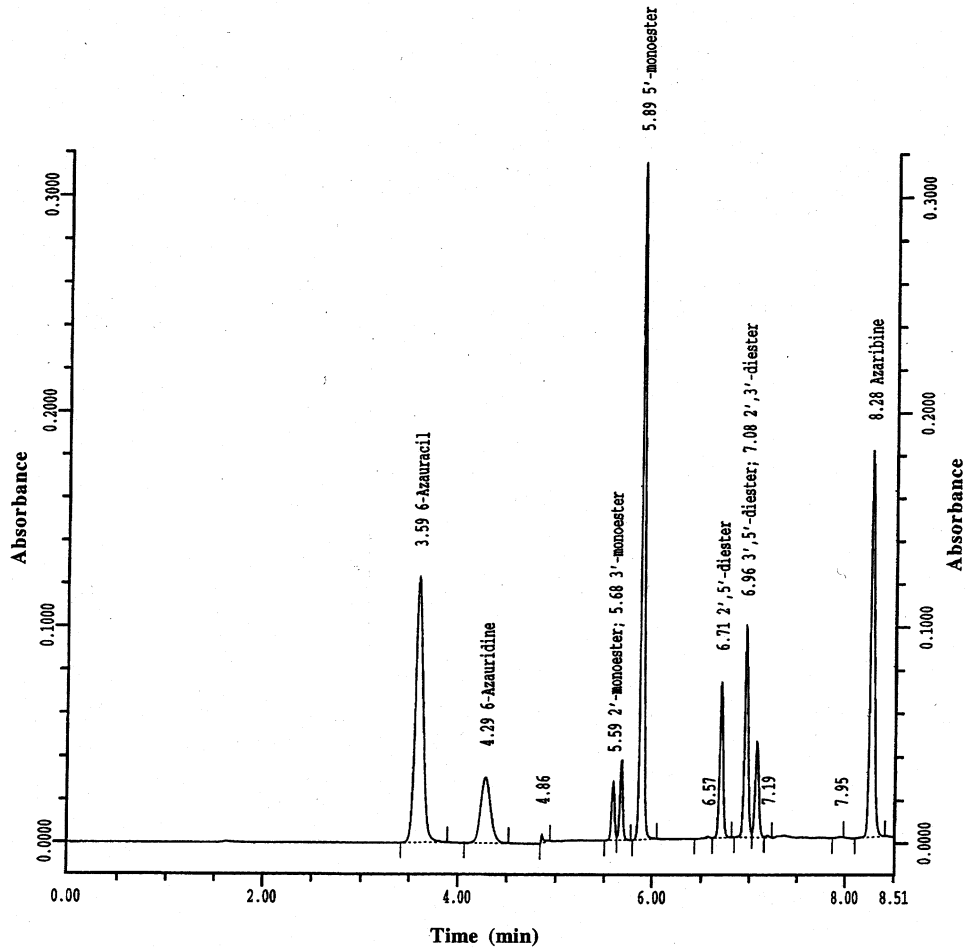

Fig. 4. LC chromatogram of the gradient separation of **1** and its metabolites. Stationary phase: ODS Hypersil column (5 μm, 150 × 4.6 mm i.d.) and guard column (5 μm, 10 × 4.6 i.d.). Mobile phase A: 100% phosphate buffer (50 mM, pH 3.00). Mobile phase B: ACN–phosphate buffer (50 mM, pH 3.00) (80:20, v/v). Gradient profile: 100% A for 0.5 min, ramp to 100% B at 8.5 min, then to 100% A at 9.5 min and reequilibrated for 5.5 min.

and **4c**) and three monoesters (**5a**, **5b** and **5c**) were present as the metabolites of **1** and no 6-azauridine appeared during the reaction time course. A simplified kinetic scheme was sought in order to fit the concentration–time profile. First, Michaelis–Menten kinetics was considered for each individual reaction step and Michaelis–Menten equation was used for each individual rate equation as shown in Eq. (4):

$$\frac{d[S]}{dt} = \frac{k_{cat}[E_t][S]}{K_M + [S]}, \quad (4)$$

where $[S]$ is the substrate concentration, k_{cat} is the catalytic rate constant (also called turnover number), $[E_t]$ is the total enzyme concentration and K_M is the Michaelis–Menten constant. Since the K_M value was very large for the disappearance of **1** (first-order reaction characteristics was observed) compared to **1** concentrations studied, an observed first-order rate constant (k_{obs}) was used to replace k_{cat} and K_M, where

$$k_{obs} = \frac{k_{cat}[E_t]}{K_M + [S]}. \quad (5)$$

The subsequent enzyme-catalyzed hydrolysis of the diesters can then also be reasoned as a first-or-

Table 1
Reproducibility of the LC gradient assay at the lowest and highest concentrations in the linearity study[a]

	1	6-Azauridine	6-Azauracil
Mean (μM)	326.7	526.5	1028
SD (μM)	0.7	0.5	3
RSD	0.2%	0.1%	0.3%
Mean (μM)	16.91	26.54	52.64
SD (μM)	0.05	0.13	0.32
RSD	0.3%	0.5%	0.6%

[a] $n = 6$ for each compound at each concentration.

der reaction due to the structure resemblance of the diesters to **1**.

Second, the hypothesis was considered that migration of an acetyl group between the 2′- and 3′-hydroxyl groups of **4b**, **4c**, **5a** and **5b** might be much faster than the deacetylation reactions so that the two pools {**4b** + **4c**} and {**5a** + **5b**} could be considered in rapid internal equilibrium. To test this hypothesis, the ratio of 2′-OAc/3′-OAc monoesters and that of 2′5′-OAc/3′5′-OAc diesters were calculated at each time point for each of the pools as shown in Table 2. These ratios, exhibited no systematic time dependence and within an

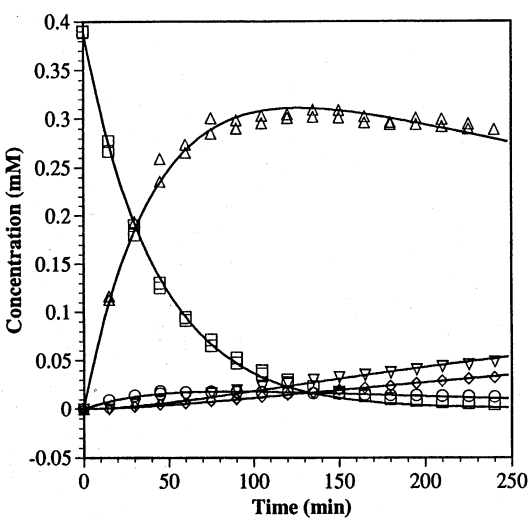

Fig. 5. Concentration-time profiles for the products of the in vitro metabolism of 2′,3′,5′-triacetyl-6-azauridine (**1**) by PLE (58.3 nM) at pH 7.50 and 30.0°C. Symbols: G, T (**1**); E, SSD (**4a**); C, PSD (**4b** + **4c**); A, PM (**5c**); S, SM (5a + 5b).

Table 2
Average ratio of 2′ Ac/3′ Ac and 2′,5′ Ac/3′,5′ Ac over the kinetic runs with PLE

	Kinetic run 1	Kinetic run 2
2′ Ac/3′ Ac	0.74 ± 0.027 (RSD: 3.6%, $n = 15$)	0.73 ± 0.019 (RSD: 2.6%, $n = 14$)
2′,5′ Ac/3′,5′ Ac	0.77 ± 0.0057 (RSD: 0.7%, $n = 16$)	0.77 ± 0.0074 (RSD: 1.0%, $n = 15$)

error of no more than 4%, were essentially constant at around 0.7–0.8 for both pairs of compounds. It was concluded that these pools are at equilibrium on the time scale of the experiments (hours) and that the equilibrium constant for conversion of 3′-OAc to 2′-OAc was 0.7–0.8.

Assuming then that the pools are in equilibrium, the kinetic system can be described (Fig. 6) as (a) conversion of the triacetate T (**1**) to SSD (**4a**) and the pool PSD (**4b** and **4c**); (b) conversion of SSD to SM, along with conversion of PSD to PM (**5c**) and SM (**5a** and **5b**). Five rate constants, k_1, k_2, k_3, k_4 and k_5 were assigned to the individual reactions as shown in Fig. 6. The time-dependencies for T, PSD, SSD, PM and SM can then be obtained by integration of the differential equations (Appendix A).

Values of the rate constants were obtained by fitting the data for each compound to the corresponding equation using Sigma Plot 4.0 software from Jandel Corporation (San Rafael, CA) on a MTech Talent 386SX125 personal computer (Microtech Computer, Inc., Lawrence, KS). Parameters for the parent compound were fitted first and used as constants in the curve fitting of the metabolites. Table 3 lists the values of the rate constants.

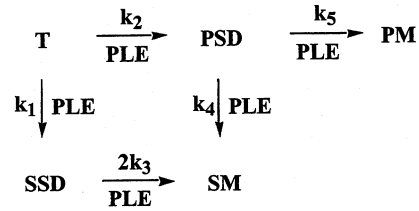

Fig. 6. Kinetic scheme for the in vitro metabolism of **1** by PLE.

Table 3
Rate constants (min^{-1}) obtained from individual curve fitting shown in Fig. 5[a]

	10^6 mean ± SE	RSD (%)	Equation[a]
k_1+k_2	24 000 ± 270	1.1	T
k_1	1600 ± 36	2.2	SSD
k_2	23 000 ± 260	1.2	PSD
k_4+k_5	1400 ± 100	7.1	PSD
k_5	530 ± 2.8	0.5	PM
k_4	560 ± 14	2.4	SM
k_3	2300 ± 120	5.0	SSD

[a] This column indicates the equation (see Appendix A) and data set (see Fig. 5) from which the parameter was obtained.

3.3. Temperature effect on **1** metabolism by PLE

The temperature effect on the rate constant of **1** in vitro metabolism by PLE (874 nM) was studied between 30.0 and 39.0°C using the fast-LC method. According to Eyring equation [9]:

$$k_{obs} = \frac{kT}{h} e^{-(\Delta H^{\neq}/RT)} e^{(\Delta S^{\neq}/R)}, \quad (6)$$

where k is the Boltzmann constant, T is the absolute temperature, h is Planck's constant, R is the gas constant, $\Delta H^{\neq}$ is the enthalpy of activation and $\Delta S^{\neq}$ is the entropy of activation. A plot of $\ln(k_{obs}/T)$ against $1/T$ gives a straight line. Fig. 7 shows a plot of $\ln(k_{obs}/T)°$ against $1/T$, where $(k_{obs}/T)°$ is the k_{obs}/T normalized to **1** M PLE. The $\Delta H^{\neq}$ (mean ± SE) obtained from this plot is 34.0 ± 3.02 KJ·mol^{-1} and the $\Delta S^{\neq}$ (mean ± SE) at 30°C calculated from this plot is −77.4 ± 9.79 J·mol^{-1}·K^{-1}, both of which are comparable with the values found for the same enzyme with other substrates [10].

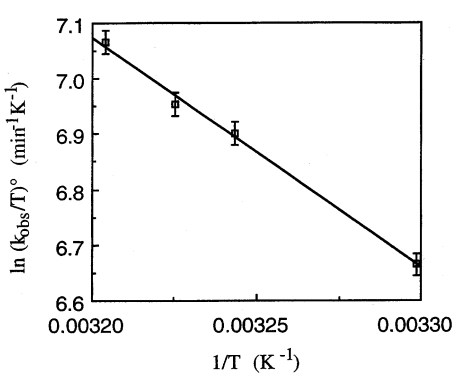

Fig. 7. The effect of temperature on the rate of in vitro metabolism of **1** by PLE (874 nM) at pH 7.50. Each experiment was conducted in duplicate.

3.4. Microdialysis sampling of **1** and its metabolites in human plasma

The application of the automated analytical system for in vitro drug metabolism studies was also demonstrated by sampling **1** and its metabolites in human plasma. Fig. 8 shows the chromatograms of: (a) a microdialysis sample of plasma without adding **1**; (b) a microdialysis sample of plasma 90 min after **1** was added; and (c) a direct manual sample of plasma without sample preparation ~345 min after **1** was added. Chromatograms (a) and (b) indicate that there was no **1** present in the plasma before spiking, and that no endogenous material interfered with the quantification of **1** or any of its metabolites by microdialysis sampling technique. A very large interfering peak was present co-eluting with the **1** when the sample was directly injected without using microdialysis or other sample preparation method as shown in chromatogram (c). This example demonstrated that microdialysis could be used not only as a sampling technique, but also as a sample clean-up method when a microdialysis membrane with appropriate molecular weight cut-off was chosen.

3.5. Kinetics of metabolism in human plasma

Fig. 9 shows the time course of the appearance and the disappearance of **1** and its metabolites in human plasma at pH 7.40 and 36.9°C. Three diesters (**4a**, **4b** and **4c**) and two monoesters (**5a** and **5b**) were present as the metabolites of **1** and no 6-azauridine appeared during the reaction time course. A negligible amount (< 0.01% of initial concentration of **1**) of 5′-monoester (**5c**) appeared after 200 min. For the same reason as with the PLE-catalyzed reaction, the hydrolysis of **1** and each of its metabolites in human plasma was considered to be first-order reaction. The ratio of 2′-OAc/3′-OAc monoesters and that of 2′5′-OAc/3′5′-OAc diesters were constant at around 0.7–0.8

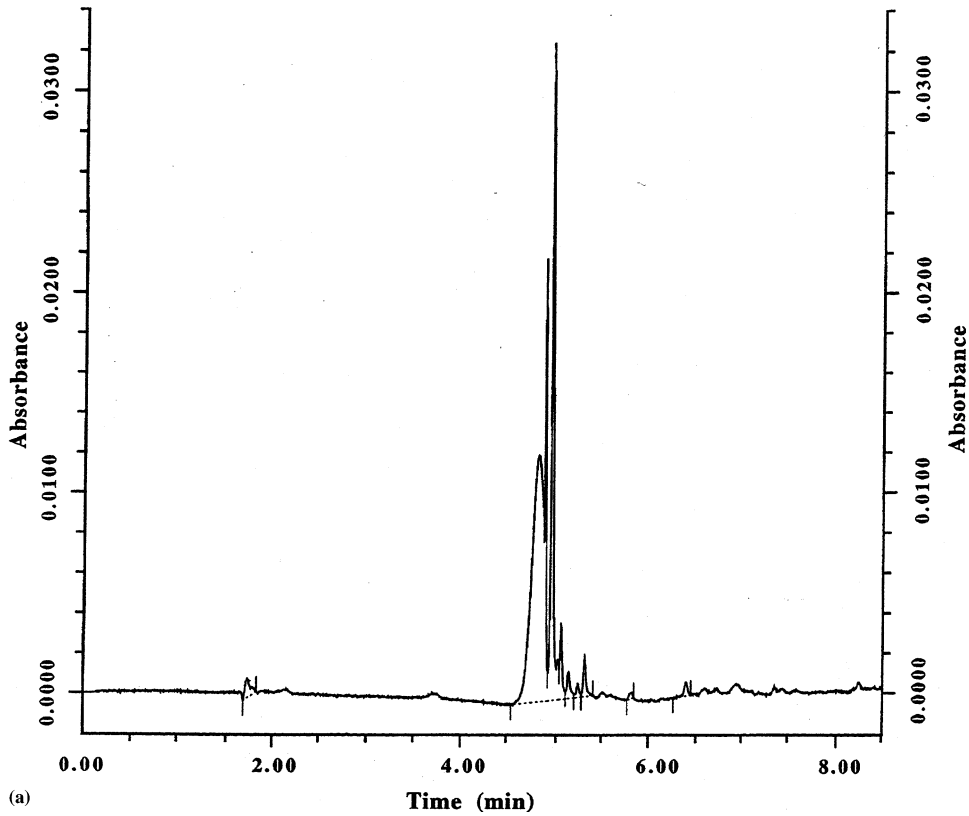

Fig. 8. (a) A gradient HPLC chromatogram of a microdialysis sample from blank plasma, conditions as in Fig. 4; (b) A gradient HPLC chromatogram of a microdialysis plasma sample 90 min after **1** was added, conditions as in Fig. 4; (c) A gradient HPLC chromatogram of a direct manually injected plasma sample without sample preparation 345 min after **1** was added, conditions as in Fig. 4.

throughout the run as shown in Table 4, indicating that the migration of the acetyl group between the 2′- and 3′- hydroxyl group of **4b**, **4c**, **5a** and **5b** was under rapid equilibrium.

Assuming that the free **1** and its metabolites are also in rapid equilibrium with their protein bound forms in human plasma, the kinetic system can be simplified (Fig. 10) to (a) conversion of the total triacetate (including free triacetate, T, and protein bound form, T-protein) to the total SSD (free SSD and SSD-protein) and the total pool PSD (free PSD and PSD-protein); (b) conversion of total SSD (free SSD and SSD-protein) to total SM (free SM and SM-protein), along with conversion of total PSD (free PSD and PSD-protein) to total SM (free SM and SM-protein). Four rate constants, k_1, k_2, k_3 and k_4 were assigned to the individual reactions as

Table 4
Average ratio of 2′ Ac/3′ Ac and 2′,5′ Ac/3′,5′ Ac inside the probe over the kinetic runs in human plasma

	Kinetic run 1	Kinetic run 2
2′ Ac/3′ Ac	0.81 ± 0.15 (RSD: 18%, $n = 22$)	0.78 ± 0.075 (RSD: 9.6%, $n = 19$)
2′,5′ Ac/3′,5′ Ac	0.70 ± 0.047 (RSD: 6.7%, $n = 23$)	0.66 ± 0.069 (RSD: 10%, $n = 21$)

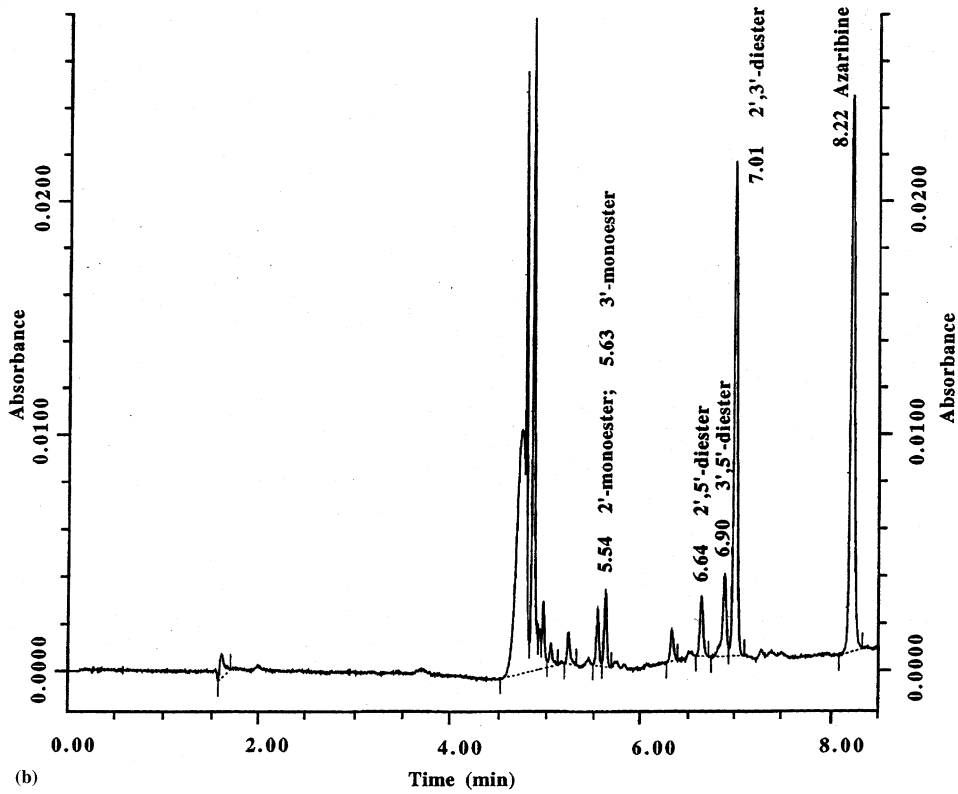

Fig. 8. (*Continued*)

shown in Fig. 10. The time-dependencies for T, PSD, SSD and SM can then be obtained by integration of the differential equations (Appendix B).

Values of the rate constants were adjusted by a combination of least-squares and manual fitting using Deltagraph Professional (Version 2.0) Software (DeltaPoint, Inc., Monterey, CA) on a Power Macintosh 7200/75 Computer (Apple Computer, Inc., Cupertino, CA) to obtain the curves shown in Fig. 9. The values of the rate constants k_1, k_2, k_3 and k_4 are shown in Table 5.

4. Discussion

4.1. HPLC assay development and validation

The gradient-LC assay was linear and reproducible for the compounds that were tested. The authentic standards of the three diesters (**4a**, **4b** and **4c**) and the three monoesters (**5a**, **5b** and **5c**) were not available at the time of study. Mummert [11] isolated and characterized these diesters and monoesters and concluded that these compounds had

Table 5
Fitness of the curves and rate constants (min^{-1}) obtained from individual curve fitting shown in Fig. 9[a]

Equation[a]	r^2	Rate constant	$\times 10^6$ min^{-1}
T	0.9976	$k_{obs} = k_1 + k_2$	7570
SSD	0.9814	k_1	6200
		$k_2 = k_{obs} - k_1$	1370
		k_3	1880
PSD	0.9001	k_4	1010
SM	0.9799		

[a] This column indicates the equation (see Appendix B) and data set (see Fig. 9) from which the parameters were obtained.

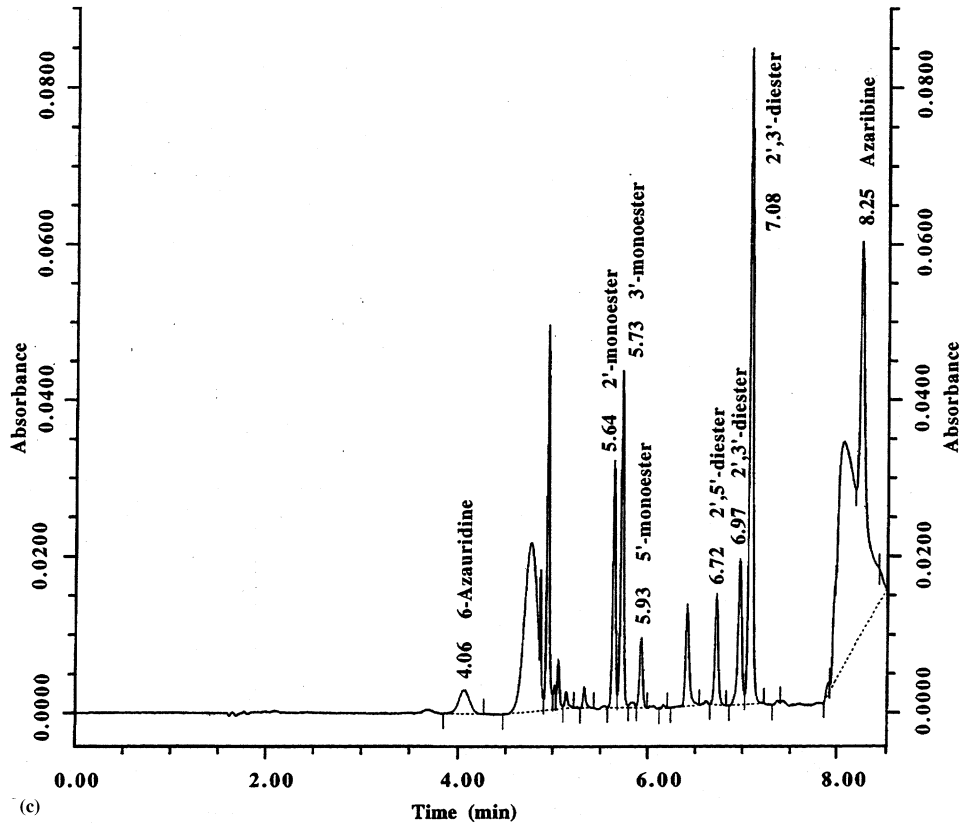

Fig. 8. (*Continued*)

similar absorptivities, and the slope values of linearity curves (of **1**, **2**, and **3**) from current study supported that claim. Hence, a calibration curve of **1** was used to convert the peak areas to the concentrations of these diesters and monoesters. The total concentration of **1** and all of its deacetylated products in PLE and human plasma catalyzed hydrolysis, calculated in this way remained constant over time, which further validated this method.

*4.2. Kinetic modeling of the in vitro metabolism of **1** by PLE*

Fig. 5 confirms that the concentration profiles for all compounds under these reaction conditions could be described by a simple kinetic model with only five adjustable parameters, the rate constants k_1, k_2, k_3, k_4 and k_5. Table 3 shows a good agreement on k_1 and k_2 from different data sets. Even for the rate constants (k_3, k_4 and k_5) determined at low concentrations ($\sim 10\%$ of the initial **1** concentration), the difference of the values obtained from different data sets was no more than 20%.

Although the deacetylation of the diesters (**4a**, **4b** and **4c**) was much slower than that of **1** in solutions with PLE, the values of the k_5 (88×10^{-7} s^{-1}), k_4 (93×10^{-7} s^{-1}) and k_3 (380×10^{-7} s^{-1}) derived from this kinetic model at pH 7.5 and 30.3°C are much larger than that of the rate constant ($P + 2S_A$, 33×10^{-7} s^{-1}) [11] for the disappearance of **1** in non-enzymatic reaction determined at pH 7.5 and 36.8°C. This comparison confirms that the hydrolysis of the diesters was catalyzed by the PLE, even though at a rate much slower than that of **1**.

The k_{obs}/A_T (mean $\pm$ SE) obtained at 58.3 nM PLE with 4% MeOH in the reaction medium was $2.6 \pm 0.03 \times 10^{-4}$ min^{-1} per unit ($n = 2$) which

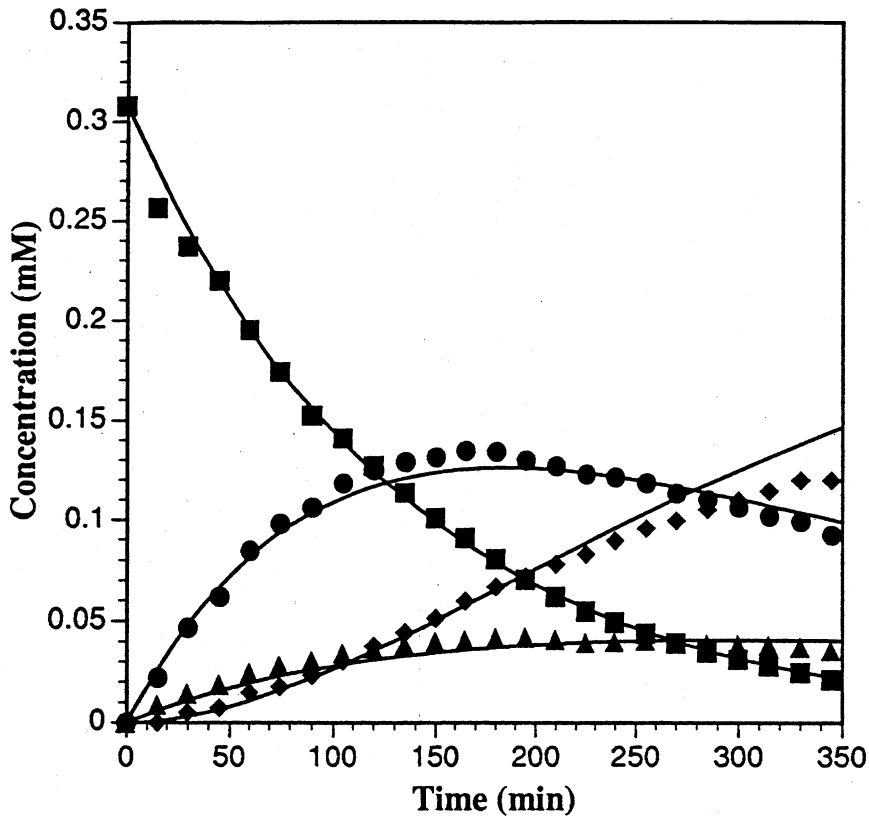

Fig. 9. Concentration-time profiles for the **1** and its metabolites in human plasma at pH 7.40 and 36.85°C. Symbols: B T (**1**); J SSD (**4a**); H PSD (**4b** + **4c**); F SM (**5a** + **5b**).

was 2.7 times larger than that reported previously [5] at 905 nM PLE with 4% MeOH ($9.7 \pm 0.4 \times 10^{-5}$ min^{-1} per unit). This discrepancy can logically be ascribed to the fact that the PLE was in different association forms. PLE can dissociate into its subunits, and when methanol is present in the solution, the subunits have higher activity than the associated molecules [12]. The lower the PLE concentration is, the more the associated PLE molecules are there, thus leading to higher activity. Table 6 shows the value of k_{obs}/A_T and its corresponding PLE concentration in different studies which further confirms the explanation.

4.3. Temperature effect on **1** metabolism by PLE

The enthalpy of activation found in the temperature effect study on **1** in vitro metabolism by PLE at pH 7.50 was 34.0 KJ mol^{-1} which was much smaller than the activation energy (98.7 KJ·mol^{-1}) [11] obtained from the non-enzymatic study at pH 7.00. Both enthalpy and entropy (-77.4 J mol^{-1} K^{-1}) of activation observed in

Table 6
A list of k_{obs}/A_T and their corresponding PLE concentrations[a]

[PLE] (nM)	10^5 k_{obs}/A_T ($n = 2$) (mean ± SD, min^{-1} per unit)	Source
58.3	26 ± 0.3	PLE kinetic modeling section
874	11 ± 0.1	Temperature effect section
905	9.7 ± 0.4[a]	[5]
1190	9.4 ± 0.6	[5]

[a] $n = 7$ for this study.

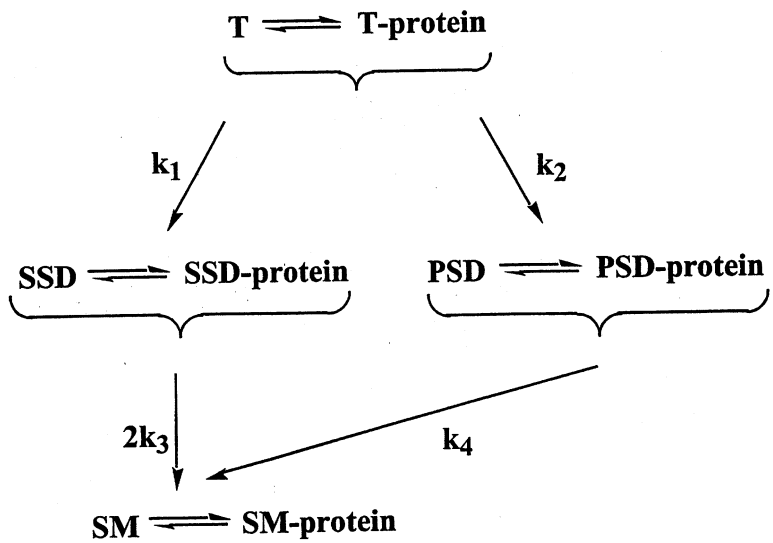

Fig. 10. Kinetic scheme for the in vitro metabolism of **1** in human plasma.

this study for PLE was comparable with those found in the literature [10] for the PLE-catalyzed hydrolysis of the separate enantiomers of methyl, phenyl, and 4-nitrophenyl 2-phenylpropionate and of the prochiral substrate dimethyl phenylmalonate ranging from 30.2 to 85.3 KJ mol^{-1} for enthalpy and from -123 to 81 J mol^{-1} K^{-1} for entropy.

*4.4. Microdialysis sampling of **1** and its metabolites in human plasma*

The kinetic study of **1** in vitro metabolism in human plasma demonstrated that microdialysis was an excellent sampling technique for the investigation of the in vitro drug metabolism in biological matrix. In this study, no sample preparation was necessary to clean up the plasma protein and other endogenous material. Microdialysis probe served as a filter to exclude almost all the macromolecules and small particulate from the samples.

Fig. 9 confirms that the concentration profiles for all compounds could be described by a simple kinetic model with only four adjustable parameters, the rate constants k_1, k_2, k_3 and k_4. The quality of the final fits shown in the figure can be judged by the correlation coefficients presented in Table 5. The model accounts for 90 to nearly 100% of the total variance for all of the four concentration-time profiles.

Table 7 shows the comparison of the normalized rate constants (NRC) between PLE and esterases in human plasma. The PLE had very high activity (NRC 96 for k_2) towards the secondary esters adjacent to an acetyl group. Even though k_3 is only 10% of k_2 in PLE-catalyzed reaction, it is more than four times larger than k_4 and k_5 in the diester hydrolysis. Instead of having a dramatic change in activity towards different substrate as shown in PLE-catalyzed reactions, activities of the esterases in human plasma generally stay in the same order of magnitude (NRC from 13 to 82) for the hydrolysis of **1** and its diester metabolites,

Table 7
Comparison of the normalized rate constants between PLE and esterases in human plasma

	PLE[a]	Human plasma[a]	Reactant and product
k_1+k_2	100	100	
k_1	6.7	82	T, SSD
k_2	96	18	T, PSD
k_3	9.6	25	SSD, SM
k_4	2.3	13	PSD, SM
k_5	2.2	0	PSD, PM

[a] The each family of rate constants were normalized by dividing each rate constant by k_1+k_2 in its own family.

except that no activity towards secondary esters adjacent to an OH group was observed. The highest activity of the esterases in human plasma was found towards the primary ester on **1**.

5. Conclusions

An automated analytical system developed previously was applied to the in vitro metabolism studies of **1** by PLE and in human plasma. Two simplified kinetic schemes were developed to describe the time course of **1**, the intermediates and final metabolites with only five and four rate constants for the metabolisms of **1** by PLE and in human plasma, correspondingly. Information derived from the kinetic models provides details of each individual metabolic step which can lead to the understanding of the mechanism of drug metabolism and/or toxicity at the molecular level. Such studies can further help to choose drug formulation type and functional group in drug design.

Acknowledgements

This work was supported by a graduate fellowship from the Kansas Health Foundation awarded to J.Z. The authors are grateful to Beckman Instruments for lending the System Gold HPLC instruments.

Appendix A. Expressions for concentrations of 1 metabolism by PLE as functions of time

T (**1**):

$$C_T = C_0 e^{-(k_1+k_2)t}$$

SSD (**4a**):

$$C_{SSD} = \frac{C_0 k_1}{(k_1+k_2)-2k_3}\left(e^{-2k_3 t} - e^{-(k_1+k_2)t}\right)$$

PSD (**4b** + **4c**):

$$C_{PSD} = \frac{C_0 k_2}{(k_1+k_2)-(k_4+k_5)}\left(e^{-(k_4+k_5)t} - e^{-(k_1+k_2)t}\right)$$

PM (**5c**):

$$C_{PM} = C_0 k_5 k_2 \left(\frac{1}{(k_1+k_2)(k_4+k_5)} + \frac{e^{-(k_4+k_5)t}}{(k_4+k_5)(k_4+k_5-k_1-k_2)} - \frac{e^{-(k_1+k_2)t}}{(k_1+k_2)(k_4+k_5-k_1-k_2)}\right)$$

SM (**5a** + **5b**):

$$C_{SM} = 2C_0 k_3 k_1 \left(\frac{1}{2k_3(k_1+k_2)} + \frac{e^{-2k_3 t}}{2k_3(2k_3-k_1-k_2)} - \frac{e^{-(k_1+k_2)t}}{(k_1+k_2)(2k_3-k_1-k_2)}\right) + C_0 k_4 k_2 \left(\frac{1}{(k_1+k_2)(k_4+k_5)} + \frac{e^{-(k_4+k_5)t}}{(k_4+k_5)(k_4+k_5-k_1-k_2)} - \frac{e^{-(k_1+k_2)t}}{(k_1+k_2)(k_4+k_5-k_1-k_2)}\right)$$

t, time; C_0, initial concentration of 2′,3′,5′-triacetyl-6-azauridine (**1**); C_T, concentration of 2′,3′,5′-triacetyl-6-azauridine at time t; C_{SSD}, concentration of SSD at time t; C_{PSD}, concentration of PSD at time t; C_{PM}, concentration of PM at time t; C_{SM}, concentration of SM at time t (see Fig. 5 and Fig. 6 for further information).

Appendix B. Expressions for concentrations of 1 metabolism in human plasma as functions of time

T (**1**):

$$C_T = C_0 e^{-(k_1+k_2)t}$$

SSD (**4a**):

$$C_{SSD} = \frac{C_0 k_1}{(k_1 + k_2) - 2k_3} \left(e^{-2k_3 t} - e^{-(k_1 + k_2)t}\right)$$

PSD (**4b** + **4c**):

$$C_{PSD} = \frac{C_0 k_2}{(k_1 + k_2) - k_4} \left(e^{-k_4 t} - e^{-(k_1 + k_2)t}\right)$$

SM (**5a** + **5b**):

$$C_{SM} = 2C_0 k_3 k_1 \left(\frac{1}{2k_3(k_1 + k_2)} + \frac{e^{-2k_3 t}}{2k_3(2k_3 - k_1 - k_2)} - \frac{e^{-(k_1 + k_2)t}}{(k_1 + k_2)(2k_3 - k_1 - k_2)} \right) + C_0 k_4 k_2 \left(\frac{1}{(k_1 + k_2)k_4} + \frac{e^{-k_4 t}}{k_4(k_4 - k_1 - k_2)} - \frac{e^{-(k_1 + k_2)t}}{(k_1 + k_2)(k_4 - k_1 - k_2)} \right)$$

t, time; C_0, initial concentration of 2′,3′,5′-triacetyl-6-azauridine (**1**); C_T, concentration of 2′,3′,5′-triacetyl-6-azauridine at time t; C_{SSD}, concentration of SSD at time t; C_{PSD}, concentration of PSD at time t; C_{SM}, concentration of SM at time t (see Fig. 9 and Fig. 10 for further information).

References

[1] R.E. Handschumacher, P. Calabresi, A.D. Welch, V. Bono, H. Fallon, E. Frei III, Cancer Chemother. Rep. 21 (1962) 1–18.
[2] R.A. Keefer, H.H. Roenigk Jr., W.A. Hawk, Arch. Dermatol. 111 (1975) 853–856.
[3] W.A. Crutcher, S.L. Moschella, Br. J. Dermatol. 92 (1975) 199–205.
[4] C.M. Riley, M.A. Mummert, J. Zhou, R.L. Schowen, D.G. Vander Velde, M.D. Morton, M. Slavik, Pharm. Res. 12 (1995) 1361–1370.
[5] J. Zhou, E.C. Shearer, J. Hong, C.M. Riley, R.L. Schowen, J. Pharm. Biomed. Anal. 14 (1996) 1691–1698.
[6] J. Zhou, R.J. Ain, C.M. Riley, R.L. Schowen, Anal. Biochem. 231 (1995) 265–267.
[7] D.J. Horgan, E.C. Webb, B. Zerner, Biochem. Biophys. Res. Commun. 23 (1966) 23–28.
[8] S.R. Knaub, M.F. Chang, C.E. Lunte, E.M. Topp, C.M. Riley, J. Pharm. Biomed. Anal. 14 (1995) 121–129.
[9] T.H. Lowry, K.S. Richardson, Mechanism and Theory in Organic Chemistry, 3rd, Harper Collins Publisher, New York, 1987, p. 209.
[10] H. Van Gelderen, J.M. Mayer, S. Cellamare, B. Testa, Chirality 6 (1994) 11–16.
[11] M.A. Mummert, in: Stability Profile of 2′,3′,5′-Triacetyl-6-azauridine, M.S. Thesis, The University of Kansas, Lawrence, KS, 1993, pp. 53–65.
[12] D. Farb, W.P. Jencks, Arch. Biochem. Biophys. 203 (1980) 214–226.